XVIII IMEKO WORLD CONGRESS
Metrology for a Sustainable Development
September, 17 – 22, 2006, Rio de Janeiro, Brazil

SOME ASPECTS OF CHROMATIC CONFOCAL SPECTRAL INTERFEROMETRY

Klaus Körner, Evangelos Papastathopoulos, Wolfgang Osten

Institut für Technische Optik, Stuttgart, Germany,
koerner@ito.uni-stuttgart.de, papastav@ito.uni-stuttgart.de, osten@ito.uni-stuttgart.de

Abstract: In this paper, we report on the recent development of a novel low coherence interferometry technique for the purpose of 3D-topography measurements. It combines the well established techniques of spectral-interferometry (SI) and chromatic-confocal microscopy (CCM). It allows for the detection of an object's depth position, without the necessity of a mechanical axial-scan, and the measurement is performed in a so-called "single-shot" manner. Focusing the white-light with a microscope objective combined with a diffractive optical element leads to an expansion of the axial-range of the sensor beyond the depth-of-focus, limited by the numerical aperture (NA) of the used objective. Confocally filtering the object's light causes the reduction of the lateral dimension of the area sampled upon the object. Due to the high NA, a high light collection-efficiency is achieved as well. The attained interferometric signals consist of high-contrast wavelets in the optical-frequency domain. The depth position of an investigated point of the object is given by the modulation-period of the wavelets. Therefore, unlike in CCM, position-wavelength referencing is not necessary.

Keywords: 3D-topography measurement, spectral interferometry, chromatic confocal microscopy.

1. INTRODUCTION

In the optical metrology, low-coherence interferometry methods like white-light interferometry (WLI) and optical coherence tomography (OCT) have attracted increasing interest for the characterizing especially of the 3D-topography of microscopic objects. Both WLI and OCT are based upon the phenomenon of low coherence interference. In these methods, the depth information is obtained by analyzing the cross-correlation pattern created during the optical interference between the low-coherent light-field reflected or scattered from an object under test and a reference field. This is typically done by mechanically scanning the optical path difference in the used interferometer and measuring the interference with a photo-detector. However, the mechanical scan is still associated to rather long duty-times. Avoiding the use of moving devices would make the sensor significantly more compact, rigid and faster. Towards this goal, different interferometry approaches have been proposed, including schemes with a tilted wavefront [1, 2] or multi-step mirrors as reference [3] as well as techniques that employ detection in the optical spectrum domain (spectral interferometry – SI), which are of particular interest within the scope of this paper.

Early approaches to SI were presented by Schwider and Zhou [4] as well as Schnell, Zimmermann and Dändlinker [5]. They observed the formation of spectral-interference fringes (also known as Müller or Tolansky Fringes), while the depth position of the investigated object was given by the modulation frequency $d\phi(k)/dk$, where $\phi(k)$ is the spectral-phase of the interference pattern and $k=2\pi/\lambda$ the wavenumber. In the following years, several approaches to SI have been reported by various authors, including the method of "spectral radar" [6] and other Fourier-domain OCT systems [7, 8], as well as unbalanced interferometers with a spectrally dispersed reference field [9, 10], and profilometers [11, 12]. One of the most distinguishing features of SI, when compared to conventional white-light interferometry sensors, is that the information about the depth-position of the investigated object is disclosed in the optical interference spectrum, experimentally acquired with a multi-channel spectrometer in a simultaneous "single shot" manner. This makes it a very promising technique for a wide variety of applications where the speed of detection plays a key role. One discrepancy encountered when applying SI for measuring the 3D-topography of microscopic objects is the limited depth range of the measurement. This is a consequence of the fact that, to retain the modulation-contrast of the interferometric signal, the axial position of the investigated object must be restricted within the depth-of-focus of the microscope objective employed for detection. This is mostly problematic in applications where high lateral resolution or high light collection efficiency are required, since focusing is performed with high numerical aperture (NA) and the axial-range of detection is limited to a few micrometers.

2. BASIC CONCEPT

Our concept utilizes a chromatically dispersed detection focus to decouple the axial depth-range of detection from the depth-of-focus. By combining the microscope objective with a diffractive optical element (DOE), the axial position of the focus varies as a function of the illumination wavelength that leads to chromatic splitting. Then, as long as the investigated object lies within the chromatically dispersed foci, due to the

light of the spectral components that are sharply focused upon the object, a high contrast interference wavelet is induced in the channelled spectrum [13]. Unlike previously reported SI schemes, the contrast of the interference signals here is independent of the numerical aperture (NA) of the microscope objective. Utilizing a high NA objective to focus allows light to be collected over a wide acceptance angle. By that, the photometric efficiency of the sensor is enhanced. Moreover, we employed a confocal pinhole to filter the light reflected or scattered from the object, similarly to the concept of chromatic confocal microscopy (CCM). This development improved the performance of the sensor in two respects: a) the size of the area sampled upon the investigated object is reduced. Therefore, the lateral resolution of the sensor is enhanced. b) The linearity of the interferometric signal is increased. In our recent letter [13], we introduced the concept of chromatically dispersed detection focus in a spectral interferometry scheme. However, one drawback encountered in these experiments was that the interference wavelets exhibited a certain amount of chirp, i.e. the modulation frequency $d\phi(k)/dk$ of the interferometric signals varied along the *k*-axis. With the new sensor design presented here, denoted as chromatic confocal spectral interferometry (CCSI) [14], the depth position of an object can be detected in a single-shot manner and without restriction of the depth range of the measurement due to the NA. Inherently the method incorporates the effective confocal filtering of the light that originate from a specific sampled focal area and suppresses signals from unfocused light-components. Due to the confocal filtering and the chromatically dispersed detection focus, CCSI interference signals occur within a much narrower spectral region, by which the uniformity of modulation frequency is retained and chirp is effectively suppressed.

3. EXPERIMENTAL SETUP

For the purpose of the experiments presented in this article, the setup depicted in Fig. 1 was employed. It consists of a Linnik-type interferometer combined with a grating-spectrometer, which is brought directly into the optical path of the outgoing light from the interferometer. The light emitted from a white-light source (Luxeon-LXHL 45 mW luminescence diode) is spatially filtered through a pinhole and subsequently collimated. The low-coherent light-field is split with a 50:50 beam-splitter-cube into two equally intense fractions, the reference and the object field. The two fields propagate along the corresponding arms of the interferometer before they are focused by two microscope objectives (Olympus 50x) of 0.8 numerical aperture (NA), identical in construction.

By inserting a diffractive optical element (DOE), a focusing Fresnel-lens with a focal length of 150 mm and a design wavelength of 630 nm, 3 mm in front of the Fourier-plane of the detection objective, the foci of the broadband illumination field are chromatically dispersed, i.e. the focal length for the "blue" part of the spectrum is longer than that for the "red" part. In contrary, the focus of the reference arm is achromatic that means no chromatic splitting is involved.

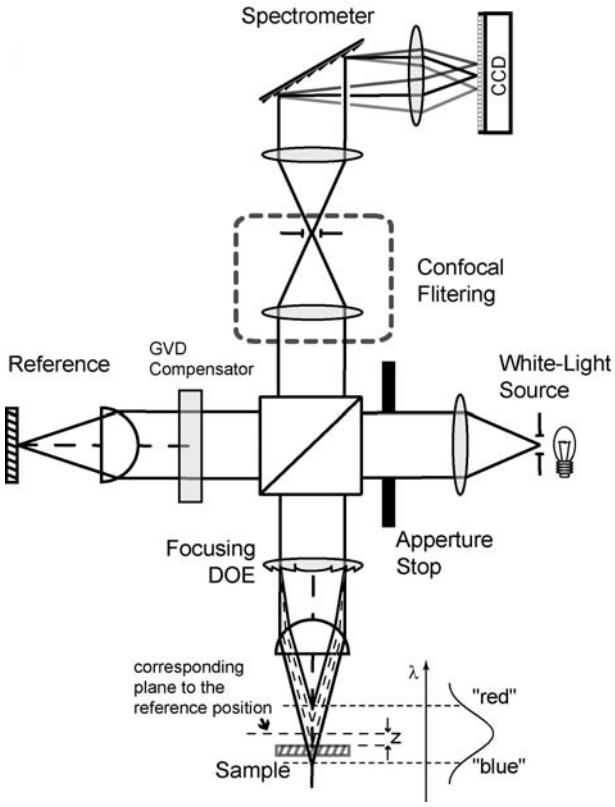

Fig. 1. Schematic representation of the white-light Linnik-type interferometer with a chromatically dispersed focus, an achromatic reference, and detection in the optical frequency domain utilizing a grating spectrometer.

Moreover, a planar quartz plate is added symmetrically to the DOE to compensate for material-dispersion (GVD) induced by the substrate of the DOE. Then, the reference field gets reflected by a flat metallic mirror which is located at the focal plane of the objective. Accordingly, the chromatically dispersed detection-field is reflected or scattered upon the surface of the investigated object. The two fields propagate backwards toward the beam-splitter-cube and recombine. In order to introduce the confocal filtering in our detection scheme, the recombined fields are focused upon a 50μm pinhole utilizing a 4x objective. Under ideal aberration-free conditions, all spectral components of the reference field are equally focused and pass effectively through the confocal pinhole. On the contrary, the light reflected from the object, due to the optical conjugation between the detection-focus and the confocal pinhole, only the spectral-components that are sharply focused upon the object will effectively pass through the pinhole and contribute to the interference signal. After that, the light passing through the pinhole is collimated and incident upon a ruled optical grating (600 lines/mm). Finally, the dispersed optical spectrum is imaged upon the chip of a CCD camera and the spectral interference signal is recorded with a laboratory computer.

4. PROOF OF PRINCIPLE EXPERIMENTS

The first proof-of-principle experiments of chromatic confocal spectral interferometry (CCSI) were performed utilizing a flat and metallic mirror as object.

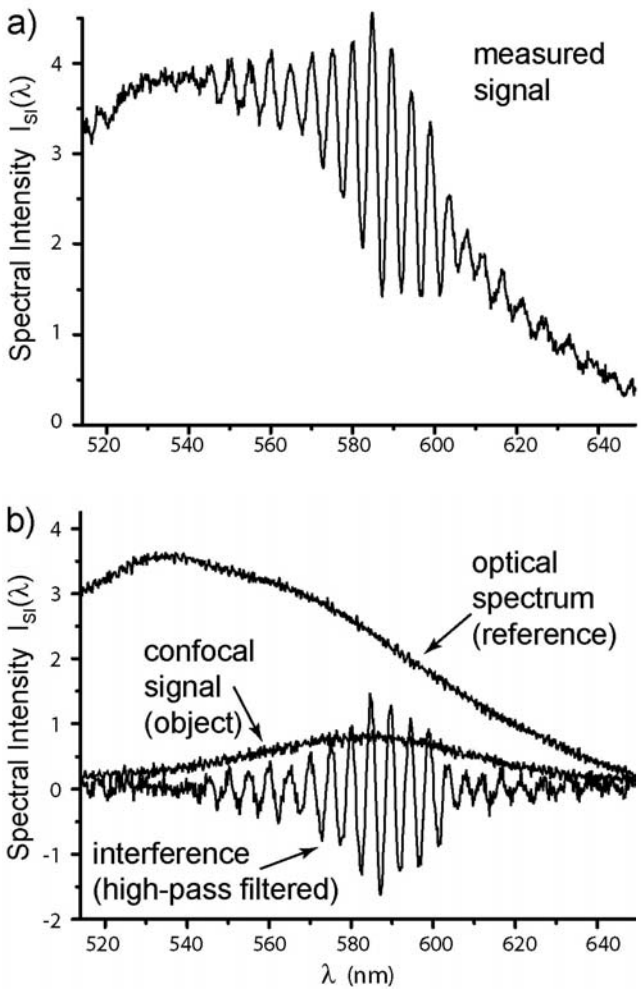

Fig. 2a. Experimentally measured interference spectrum involving a 0.8 NA microscope objective and a 50 µm confocal pinhole. Fig. 2b. The individual spectra of the reference and object fields are depicted (upper and middle curves respectively). The interference wavelet of the lower curve results from high-pass filtering the measured signal in Fig. 2a.

For a fixed position of the object, we measured the channelled interference spectrum shown in Fig. 2a. For a fixed position of the object, we measured the channelled interference spectrum shown in Fig. 2a. It exhibits an interference wavelet confined within a spectral range of ~40 nm and centered on a central wavelength λo=585 nm. The modulation-amplitude of the interference amounts to 50% of the entire signal. In order to investigate the role of confocal filtering, the spectral contributions from the two individual reference- and object-fields were measured by sequentially opening the respective arms of the interferometer. The upper curve in Fig. 2b shows the contribution from the reference-field while the object-field is blocked. It coincides with the optical spectrum of the white-light source employed and exhibits a smooth varying profile; it is centered on 530 nm and has a bandwidth of ~120 nm. In the same graph, the confocally filtered contribution of the object-field (reference-field is now blocked) is also shown, indicated as "confocal signal". This signal is directly comparable to measurements performed following the method of chromatic confocal microscopy, previously reported by a number of authors [15-19] and can be as well used to acquire the axial z-position of the object in a single-shot manner. This is achieved by finding the central wavelength where the modulation of the spectral signal is maximal (maximal contrast detection). Then, by means of a reference measurement, an axial-position is assigned to this wavelength (Focus-Wavelength-Encoding). However, with CCSI this position-wavelength referencing is not necessary. Detection of the object's z-position is here realized by monitoring the modulation frequency of the spectral interference signal $z = 1/2 \cdot d\phi(k)/dk$ [13]. Therefore, a wavelength referencing of the channelled spectrum is sufficient for the z-calibration. This was performed with superb accuracy utilizing a low-cost discharge lamp.

As next step, the interference spectrum was measured for different z-positions of the object. This was experimentally realized by displacing the object with a micrometric z-driver. The emerging high-pass filtered interference wavelets are accordingly summarized in Fig. 3a. Since we are interested in the modulation frequency of the interferograms that is given by spectral-phase gradient $d\phi(k)/dk$, the representation in the wavenumber k=2π/λ domain is here rather employed. All wavelets in Fig. 3a exhibit practically equidistant fringe spacing. This clearly demonstrates that in contrast to our previously reported results [13], the interference signals acquired with the CCSI sensor are practically unchirped. On the light of this finding, a fast Fourier transformation (FFT) was applied to the interference signals in order to retrieve the axial position of the object. The z values acquired from this analysis are indicated at the upper-left side of each graph in Fig. 3a.

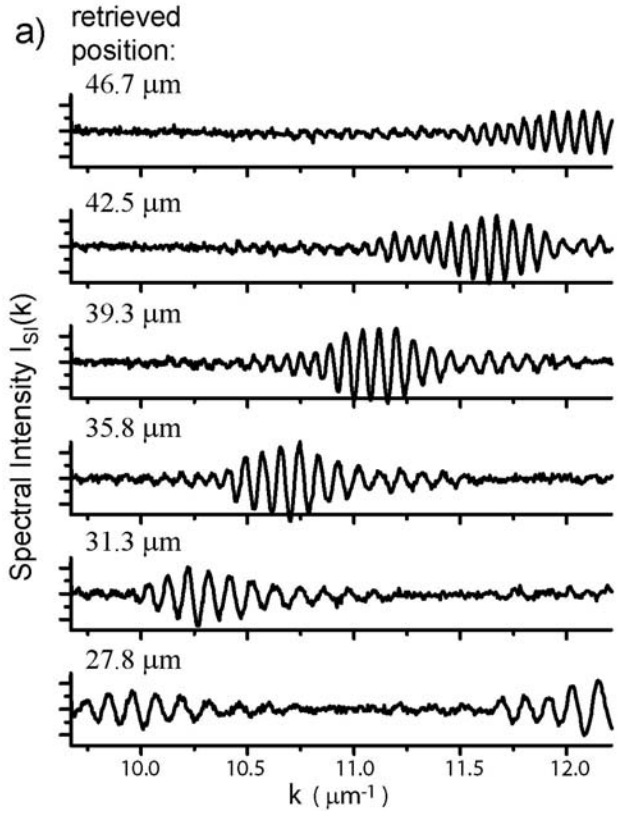

Fig. 3a. Experimentally measured and high-pass filtered interference wavelets for various axial positions of the reflecting object.

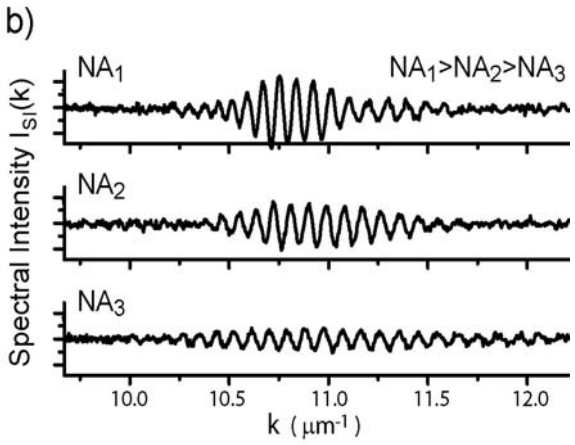

Fig. 3b. Experimental investigation of the effect of numerical aperture upon the CCSI signals. The interference wavelets above (high-pass filtered) were measured for various diameters of the aperture-stop of the illumination field and a constant object z-position.

Interestingly, in the lower frame of Fig. 3a, a second wavelet appears at the right side of the graph. The origin of this interference is presumably a higher order diffraction focus from the DOE. Its modulation frequency coincides with that of the wavelet on the left side of the graph. This observation diminishes the possibility that the second wavelet originates from a higher order diffraction of the spectrometer grating. Also the assertion that this interference could be due to a reflection from an intermediate optical surface in the setup can be safely excluded, since on one hand, both the position and the carrier-frequency of the wavelet are z-dependent, on the other hand an intermediate reflection would propagate through a different optical path and contribute with a different modulation frequency to the interference spectrum. By further displacement of the object, the first-order interference wavelet is no longer in the range of the spectrometer. However, the second-order wavelet was utilized to expand the axial range of the detection scheme over 40 μm.

5. VARIATION OF THE NUMERICAL APERTURE

The parameter which mostly influences both the lateral- as well as depth-resolution of the CCSI sensor is the numerical aperture (NA) of the detection focus. The experimentally most easily accessible way to influence the (effective) NA, without significantly disrupting the alignment of the system is by changing the diameter of the aperture stop depicted in Fig. 1. Accordingly, the effect of the NA variation upon the generated signals was investigated by recording the interference wavelets for three different values of the aperture stop diameter.

The resulting high-pass filtered wavelets are summarized in Fig. 3b. It is evident that for a decreasing stop-diameter and respectively smaller numerical aperture, the interference wavelets become spectrally broader. Within the CCSI concept, this effect is well incorporated, since for smaller NA the depth-of-focus becomes longer. As a result, a larger range of the chromatically dispersed foci becomes sharply focused upon the object and the high-contrast modulation condition is fulfilled for a broader part of the white-light spectrum. Furthermore, since the emitted intensity from the employed white-light source was kept constant during this experiment, the light reaching the CCD camera is also reduced for the smaller stop-diameters. This causes the amplitude of the interference wavelets in Fig. 3b to undergo a relative decrease as the NA becomes smaller. This photometric effect influences equally the intensities of both the reference- as well as the object-field and therefore had no influence upon the contrast of the interference signal.

6. MEASUREMENTS ON TECHNICAL OBJECTS

The motivation of this work was mainly the development of a method, which could provide solutions for a variety of technical optical metrology problems. Accordingly, we employed our Linnik-based CCSI prototype to perform topography measurements on some objects of technical interest. The first investigated object was a mechanically face-ground machined metallic surface (Fig. 4c). It comprises a planar reference sample with a known roughness constant R_a=2.5 μm. The definition of R_a is schematically summarized in Fig. 4b. A common problem encountered in interferometric measurements upon such objects is the degradation of phase information of the interference signals.

Due to the stochastic complexity of the object's surface, the area sampled by the detection field encloses a variety of sub-planes with a diverse depth distribution. The interference pattern induced by each sub-plane exhibits a phase structure which respectively varies across the optically sampled area. For this, the measured interference signal, which is the sum of all sub-plane contributions, exhibits also a significantly complex phase structure. In the measurement presented here this discrepancy was lifted by employing a high numerical aperture 0.8 NA objective (without restriction of the depth-range of the measurement). Due to the tightly focused detection-field and the confocal pinhole, a small area upon the object's surface could be sampled with a high lateral resolution. Therefore, the phase information of the acquired interference wavelets was retrieved, despite the comparatively large roughness of the investigated object. The measured signal is depicted in Fig. 4a where the contrast of modulation amounts to over 25%.

As a next step, the object depicted at the lower-right graphic in Fig. 5 was examined utilizing the CCSI Linnik-setup. It comprises a laser-processed Wolfram plate and is a courtesy of the company TRUMPF. Compared to the previous sample, this object exhibits a lower reflectivity and an unknown roughness. The sub-frame upon the logotype shown in right-top graph in Fig. 5 exhibits a step structure which was sampled within the marked areas A and B. The recorded and high-pass filtered wavelets are accordingly depicted at the left of Fig. 5. It has to be noted that the signal B comprises a second order interference wavelet, mentioned in the previous section. Both measurements exhibit well defined phase structures, the Fourier transformation of which were utilized to retrieve the position of the sampled areas. The contrast of the interferometric signals both for the laser-processed plate as well as the face-ground machined metal surface are influenced by the relative intensities of the

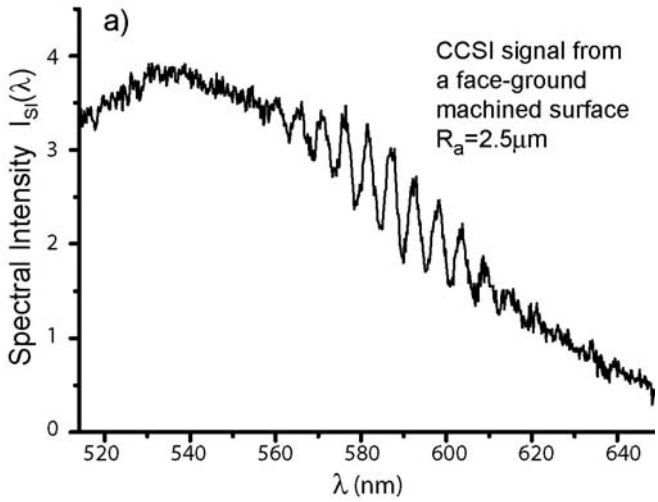

Fig. 4a. Experimentally acquired interference wavelet involving CCSI measurement on a mechanically face-ground machined surface with a referenced roughness R_a=2.5 µm.

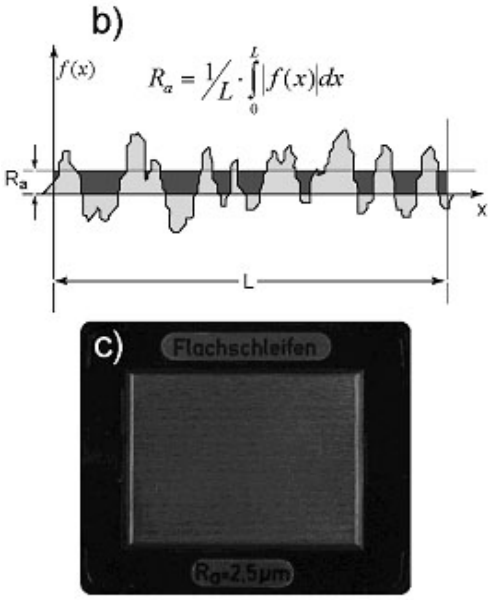

Fig. 4b. Schematic representation of the definition of the roughness constant R_a . Fig. 4 c. Photograph of the investigated sample.

reference and object fields. The use of a high-NA objective here features a significant advantage of the method, since light from a wide acceptance angle is collected, increasing respectively the photometric sensitivity of the sensor. The contrast of these interferograms could be further increased by reducing the intensity of the reference field which in the above measurements was kept constant; the reference surface was in all measurements a flat metallic mirror.

7. CONCLUSION

The method of chromatic confocal spectral interferometry (CCSI) is a hybrid technique which allows for white-light interferometric detection with high numerical aperture (NA) in a single-shot manner. The present work

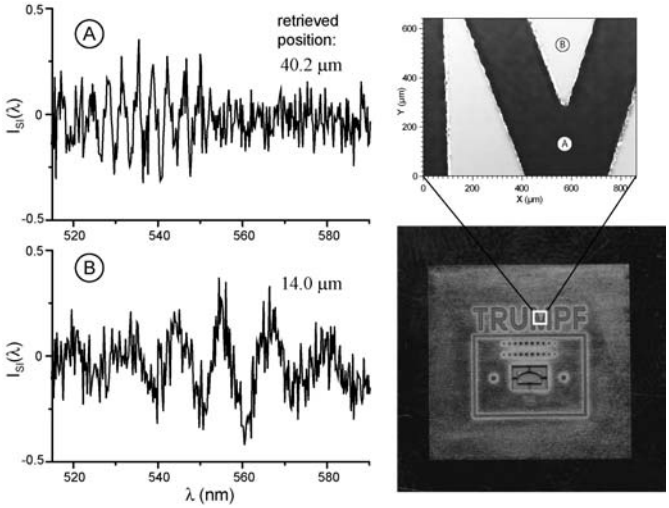

Fig. 5. Experimentally acquired interference wavelets (A and B) involving a laser-processed Wolfram plate. This object is courtesy of TRUMPF. It exhibits a step structure which was measured by monitoring the modulation frequency of the interference signals from the sampled areas A and B.

contributes to the emerging trend of employing spectral detection for the purposes of 3D-topography measurements.

By utilizing the "fourth" spectral dimension, mechanical depth-scan of the sensor is no longer necessary. This opens many new possibilities for optical detection with dramatically reduced duty-time and for enhancing the robustness of the sensor.

To our knowledge, CCSI is the first interferometric method which utilizes a confocally filtered and chromatically dispersed focus for detection, and on the other hand, allows for retrieval of the depth position of reflecting or scattering objects, utilizing the phase (modulation frequency) of the interferometric signals acquired. The chromatically dispersed focus allows for decoupling the depth range of the sensor from the NA of the microscope objective. Consequently, by use of a high NA detection focus, both the lateral resolution as well as the photometric sensitivity of the sensor are enhanced.

Moreover, with the phase detection strategy employed here, the depth resolution of the sensor is enhanced. Compared to the sensor presented in our recent letter [13], we implemented here a more effective confocal filtering which has enhanced the phase-linearity of the interferometric signals acquired (chirp suppression). By this, a fast Fourier transformation strategy could be employed to acquire the axial-position of the object, while unlike in previously reported topography sensors that utilize the chromatic concept, with CCSI no position-wavelength referencing is necessary. In the present communication, the principles of this new interferometry method were experimentally shown.

Finally, on the basis of topography measurements performed upon two technical objects, the applicability of the method for optical detection of objects with rough surfaces and limited reflectivity was demonstrated.

REFERENCES

[1] Y. Yasuno, S. Makita, T. Endo, G. Aoki, H. Sumimura, M. Itoh, and T. Yatagai, “One-shot-phase-shifting Fourier domain optical coherence tomography by reference wavefront tilting”, Opt. Express 12, pp. 6184-6191, 2004.

[2] M. Hering, S. Herrmann, M. Banyay, K. Körner, B. Jähne, “One-shot line-profiling white-light interferometer with spatial phase shift for measuring rough surfaces”, Proc. SPIE 6188, pp. 14-24, 2006.

[3] C. Bosbach, F. Depiereux, T. Pfeifer, B. Michelt, “Fiber-optic interferometer for absolute distance measurements with high measuring frequency”, Proc. SPIE 4900, pp. 408-415, 2002.

[4] J. Schwider, L. Zhou, “Dispersive interferometric profilometer”, Opt. Lett. 19, pp. 995-997, 1994.

[5] U. Schnell, E. Zimmermenn and R. Dändliker, “Absolute distance measurement with synchronously sampled white-light channelled spectrum”, Pure Appl. Opt. 4, pp. 643-651, 1995.

[6] M. Bail, G. Häusler, J. M. Herrmann, M. W. Lindner, R. Ringler, “Optical coherence tomography with the "Spectral Radar" -Fast optical analysis in volume scatterers by short coherence interferometry”, Opt. Lett. 21, pp. 1087-1089, 1996.

[7] M. Wojtkowski, R. Leitgeb, A. Kowalczyk, T. Bajraszewski, A. F. Fercher ,”In vivo human retinal imaging by Fourier domain optical coherence tomography”, J. Biomed. Opt. **7**, pp. 457-463, 2002.

[8] T. Endo, Y. Yasuno, S. Makita, M. Itoh, T. Yatagai, “Profilometry with line-field Fourier-domain interferometry”, Optics Express 13, pp. 695-701, 2005.

[9] P. Pavlicek, G. Häusler, “White-light interferometer with dispersion: an accurate fiber-optic sensor for the measurement of distance”, Appl. Opt. 44, pp. 2978-2983, 2005.

[10] P. Hlubina, “Dispersive white-light spectral two-beam interference under general measurement conditions”, Proc. SPIE Vol. 5259, pp. 281-288, 2003.

[11] J. Calatroni, A. L. Guerrero, C. Sainz and R. Escalona, “Spectrally-resolved white-light interferometry as a profilometry tool”, Opt. & Laser Tech. 28, pp. 485-489, 1996.

[12] P. Sandoz, G. Tribillon and H. Perrin, “High-resolution profilometry by using phase calculation algorithms for spectroscopic analysis of white-light interferograms”, J. Mod. Opt. 43, pp. 701-701, 1996.

[13] E. Papastathopoulos, K. Körner and W. Osten, “Chromatically dispersed interferometry with wavelet analysis“, Opt Lett. 31, pp. 589-591, 2006.

[14] E. Papastathopoulos, K. Körner and W. Osten, “Chromatic Confocal Spectral Interferometry (CCSI)“, submitted to Appl. Opt.

[15] G. Molesini, G. Pedrini, P. Poggi and F. Quercioli, “Focus-wavelength encoded optical profilometer”, Opt. Commun. 49, pp. 229-233, 1984.

[16] M. A. Browne, O. Akinyemi, A. Boyde, “Confocal surface profiling utilizing chromatic aberration”, Scanning 14, pp. 145-153, 1992.

[17] H. J. Tiziani, H. M. Uhde, “Three dimensional imaging sensing by chromatic confocal microscopy”, Appl. Opt. 33, pp. 1838-1843, 1994.

[18] S. L. Dodson, P. C. Sun and Y. Fainman, “Diffractive lenses for chromatic confocal imaging”, Appl. Opt. 36, pp. 4744-4748, 1997.

[19] S. D. Cha, P. C. Lin, L. J. Zhu, P. C. Sun, Y. Fainman, “Nontranslational three-dimensional profilometry by chromatic confocal microscopy with dynamically configurable micromirror”, Appl. Opt. 39, pp. 2605-2613, 2000.